

Electroacupuncture Improves Neurogenic Bladder Dysfunctions in Spinal Cord Injury Rat Model by Regulating BDNF-TrkB and MAPK Signaling Pathways

YUEBO JIANG, YING LI¹, XIAOYAN SONG², ZONGYUE HUANG³, MIAOMIAO LI¹, XINXIN XIAO³ AND LING GUAN*

Department of Acupuncture and Moxibustion, The Sixth Medical Center of People's Liberation Army General Hospital and Medical School, Beijing 100037, ¹The First Medical Center of Chinese People's Liberation Army General Hospital and Medical School, Beijing 100853, ²Department of Cadre Diagnosis and Treatment, The Eighth Medical Center of People's Liberation Army General Hospital, Beijing 100091, ³The First Medical Center of Chinese People's Liberation Army General Hospital and Medical School, Beijing 100853, China

Jiang *et al.*: Neurogenic Bladder Dysfunctions in Rat Spinal Cord Injury by Electroacupuncture

To explore protective effects and possible electroacupuncture mechanisms on neurogenic bladder dysfunctions in a spinal cord injury rat model. Forty-eight spinal cord injury model rats were prepared using modified Allen's method and then randomly assigned to the sham operation group, model group and treatment group, and the healthy Sprague-Dawley rats were used as controls. After 7 d of electroacupuncture intervention, the minimum contraction tension and contraction frequency of isolated detrusor strips in each group were measured. At the end of the experiment, rat bladders were taken for histopathological analysis and detection of protein and messenger ribonucleic acid levels of proinflammatory factors. Reverse transcription-polymerase chain reaction and Western blotting methods were also applied to measure the levels of messenger ribonucleic acid and protein associated with brain-derived neurotrophic factor-tyrosine kinase B and mitogen-activated protein kinase signaling pathways, respectively. Treatment of electroacupuncture could significantly improve Basso-Beattie-Bresnahan limb motor function score in spinal cord injury model rats. Reverse transcription-qualitative polymerase chain reaction and enzyme-linked immunosorbent assay results showed that electroacupuncture treatment exhibited a statistical decrease in the expression of proinflammatory factors in the bladder tissues of spinal cord injury model rats relative to the spinal cord injury control group. In addition, the Western blotting results showed that electroacupuncture treatment significantly up-regulated the brain-derived neurotrophic factor/tyrosine kinase B pathway and significantly inhibited the activation of mitogen-activated protein kinase inflammation-related signaling pathways relative to the model control group. Electroacupuncture can ameliorate neurogenic bladder dysfunctions in the spinal cord injury rat model by regulating brain-derived neurotrophic factor-tyrosine kinase B and mitogen-activated protein kinase signaling pathways.

Key words: Electroacupuncture, spinal cord injury, brain-derived neurotrophic factor, tyrosine kinase B, mitogen activated protein kinase, neurogenic bladder dysfunction

Spinal Cord Injury (SCI) refers to a type of disease in which traumatic violence acts on the spine and causes spinal fracture and dislocation, leading to spinal cord and cauda equine damage, and motor function, sensory function, nerve reflexes and sphincter dysfunction in the limbs below the level of injury^[1,2]. The pathophysiological response of SCI is very complex, including a cascade caused by a series of causes such as spinal cord edema, ischemia, inflammatory response, and cell necrosis,

which eventually leads to SCI, and these causes can also seriously affect axonal repair and limb function recovery after SCI^[3,4]. Until now, no ideal treatment for SCI^[5,6]. Moreover, common complications such as micturition disorders occur after SCI, i.e. urinary incontinence caused by neurogenic bladder, hydronephrosis, and urinary tract infection^[7]. These complications develop to a later stage and will be accompanied by chronic renal failure, which may lead to patient death in severe cases, bringing a

*Address for correspondence
E-mail: guanling301@sina.com

heavy burden to patients and their families and even society^[8].

At present, although there have been many therapeutic studies on SCI, there has been no substantial progress in improving neurological function or promoting neurological recovery, mainly because it is difficult to find targeted interventions to control primary injury and a series of vascular, cellular, and biochemical reactions induced later leading to secondary damage^[9,10]. Therefore, as there are unmet medical needs, finding more effective and safer therapeutic agents or measures is an important direction to promote neurological recovery research in SCI. Brain-Derived Neurotrophic Factor (BDNF) is also one of the abundant neurotrophins and is widely distributed in the Central Nervous System (CNS)^[11,12]. A recent study showed that BDNF binds to its high-affinity Tyrosine Kinase B (TrkB) receptor (BDNF/TrkB) after SCI and can promote neural cell survival, axonal growth, and synaptic plasticity, thereby promoting axonal repair and limb motor function recovery after SCI^[13,14]. Therefore, BDNF/TrkB signaling expression has emerged as a research hotspot for axonal regeneration and repair after SCI. Mitogen-Activated Protein Kinase (MAPK) is a series of serine-threonine protein kinases that can be activated by cytokines, neurotransmitters, hormones, cellular stress, and cell adhesion^[15-17]. MAPK signaling pathway is often detected by three indicators; Extracellular Signal-Regulated Kinase (ERK), p38 MAPKs, and c-Jun N-Terminal Kinase (JNK). P38 MAPK is activated after cell injury stress and activates a series of signaling pathways and proteins downstream of inflammation; injured spinal cord neurons, astrocytes, and macrophages increase the expression of p38 MAPK, and down-regulation of p38 MAPK expression after SCI can promote SCI functional recovery^[18,19]. Similar to p38, JNK is also involved in the process of inflammation development and cell death, and inhibition of JNK expression contributes to the recovery of CNS injury, and inhibition of JNK expression after SCI contributes to functional recovery after SCI^[20].

In this study, Electroacupuncture (EA) was proposed to intervene in the SCI rat model to observe its effect on promoting the recovery of neurological function in acute SCI rats and to explore whether the possible mechanism of acupuncture is related to MAPK and BDNF/TrkB signaling pathways, and its action mechanism.

MATERIALS AND METHODS

Development of SCI rat model:

The experimental animals selected for this study were Specific-Pathogen-Free (SPF) Sprague Dawley (SD) rats, (8-10) w old, and all female, weighing (200±15) g. Experimental rats were purchased from Shanghai Slack Laboratory Animal Co., Ltd., (Shanghai, China). All animals were housed in SPF grade laboratory animal center on a rat columnar pellet standard diet provided by the Laboratory of Animal Center at Chinese People's Liberation Army (PLA) medical school. The room temperature was 20°-25°; the relative humidity was 55 %-65 %, and the light duration was about 12 h daily, 5 animals/cage, with plastic water bottles and stainless steel water absorption tubes. The animals had free access to food and water, and the bedding was changed every 3 d. After the animals were placed in the feeding room, they rested for (5-7) d to adapt to the environment. All the rat care and the subsequent surgical procedures were according to the instructions of the Sixth Medical Center of Chinese PLA General Hospital and Medical School. They were permitted by the Ethics Committee for Research on Animal Use in Laboratory Experiments.

Modified Allen's SCI modeling method was used to construct the model rats^[21]. The detailed steps were as follows; after weighing, the lower abdominal injection area was disinfected with 2 % iodine tincture, and 75 % alcohol deiodination was used to anesthetize the rats intraperitoneally with chloral hydrate at 3.5 ml/kg. After the rats breathed steadily and had no corneal reflex, the rats were fixed; by touching the ribs and spinous processes, the spinous processes of the thoracic spine of T10 were located as the center, a longitudinal skin incision of about 4 cm was cut, and the subcutaneous tissues were cut in turn to expose the spinous processes of T10, and adequate hemostasis was performed; forceps were used to expose the spinal canal from the laminar space, fully expose the spinal cord, and then 3.5 mm round thin plastic gaskets were placed on the surface of the spinal cord of T10, and a modified Allen's device was used to freely drop 10 g of the weight from 3.5 cm height, which impacted the dural sac, resulting in T10 spinal cord impact injury. After successful modeling, penicillin 2×10 U was intraperitoneally injected to prevent wound and urinary tract infection.

Grouping and intervention of model animals:

SD rats were divided into four groups: Control group has no modeling treatment and blank control; sham operation group has only skin and other soft tissues were incised without transection of the spinal cord; model group has SCI was treated with acupuncture after successful modeling and EA group has Huatuo brand 0.25×25 mm acupuncture needle was used to acupuncture Ciliao and Zhongliao points (located in the inferomedial aspect of the posterior superior iliac spine of the sacral region at the 2nd and 3rd sacral hiatus) in rats and EA stimulation parameters were connected with EA therapeutic apparatus (Huatuo brand EA instrument) after inserting the needle de qi; the frequency of sparse waves was 10 Hz, the intensity was mild limb tremors, and the needle was removed and pressed to stop bleeding 20 min after retaining EA. The process was done once daily for 7 d.

Basso-Beattie-Bresnahan (BBB) score:

At 7 d and 14 d after surgery, rats from each group were randomly selected for BBB scoring^[22]. Scoring was performed independently by non-group experimenters familiar with the scoring criteria of this experiment and observed for 5 min. Then, the rat was measured three times and averaged. Rats drawn before scoring had their bladders checked for filling to avoid compromising scoring results due to bladder filling.

Improvement assessment for urinary and stool disorders:

Urodynamic studies included maximum bladder capacity measurements and filling intravesical pressure measurements as described previously^[23]. The determination method of maximum bladder capacity can be briefly elucidated as follows; after maneuver-assisted rat urination, the rat was fixed on the operating table, two catheters were filled with warm normal saline and inserted into the bladder, the lower abdomen of the rat was gently pressed to discharge urine along one catheter, after no urine outflow, 37° normal saline was injected into the bladder at a rate of 0.1 ml/s through a red graduated catheter, and when there was a fluid overflow, the injected normal saline capacity was the maximum bladder capacity of the rat. Maximum bladder capacity was measured in the conscious state of rats on d 14 after surgery and d 1 after 7 treatments.

Filling intravesical pressure: After rats were anesthetized with 0.5 % hydrochloride, the bladder was exposed after cutting a 3 cm wound, and a scalp needle was punctured into the bladder fornix as a cystometric tube, purse-string suture of the seromuscular layer was performed, and the manometric tube was connected to the urodynamic instrument and a micro perfusion pump through a three-way tube, respectively. The bladder was instilled with normal saline at a rate of 0.1 ml/s for filling cystometry to simulate the pressure change during the urinary phase. The bladder pressure change curve was recorded, the leakage point pressure was recorded, and the intravesical pressure filled intravesical pressure when continuous leakage occurred at the urethral meatus. Bladder compliance was calculated based on bladder compliance equal to the ratio of changes in perfusion volume to changes in bladder pressure.

Western Blot (WB) analysis:

At the endpoint, the rats in all groups were sacrificed by cervical dislocation, bladder tissues were rapidly isolated immediately and kept on ice, and three samples from each group were used for WB investigation^[24]. Rabbit anti-rat BDNF/TrkB/p38 MAPK/Glyceraldehyde 3-Phosphate Dehydrogenase (GAPDH) monoclonal antibody and other antibodies, and Enzyme-Linked Immunosorbent Assay (ELISA) kits were brought from ABCAM (United States of America (USA)). Anti-Alexa Fluor 688 fluorescent secondary antibody was obtained from Thermo Fisher (USA).

Following the rapid placement of bladder tissue samples into a centrifuge tube, 1 ml of cell lysate and 10 µl of Phenylmethanesulfonyl Fluoride (PMSF) storage solution were added per 100 mg of tissue. The mixture was then completely ground, and the protein concentration was determined using the Coomassie brilliant blue method. The sample protein was loaded from each tissue and transferred to a Polyvinylidene Fluoride (PVDF) membrane using 10 % Sodium Dodecyl Sulphate-Polyacrylamide Gel Electrophoresis (SDS-PAGE) after being heated at 100° for 5 min. After being blocked with 5 % Bovine Serum Albumin (BSA), the primary antibodies (1:1000) were applied and left overnight at 4°. Membranes were treated three times with Tris-Buffered Saline with 0.1 % Tween® 20 Detergent (TBST) before being incubated with secondary antibodies (1:2000) labeled with horseradish peroxidase

for 1 h at room temperature. After a 1 min reaction, color development was made in the dark, coated with PVDF membranes, and photographed. The gel imaging system utilized was from ODYSSEY-FC (LiCor, USA). Image-lab software was used to calculate and analyze the optical density of protein bands.

Reverse Transcription-qualitative Polymerase Chain Reaction (RT-qPCR) analysis:

RT-qPCR was used to measure gene expression levels of Interleukin-1 Beta (IL-1 β), IL-6, Tumor Necrosis Factor-Alpha (TNF- α), and genes of signaling pathways^[24]. At the detection point, the selected rats from each group were randomly selected and 0.5 cm cephalad and caudal spinal cord tissues centered on the injury point were taken. Total Ribonucleic Acid (RNA) was extracted using the Trizol reagent by following its protocol (Invitrogen, USA). After detecting the RNA concentration and purity, complementary Deoxyribonucleic Acid (cDNA) was synthesized from 1 μ g of total RNA using the PrimeScript™ RT reagent Kit (RR047A, Clontech Takara Bio INC, Japan) by placing reaction samples in the T100™ PCR instrument (Bio-RAD, USA) for reverse transcription. The successive cDNA was utilized for RT-qPCR using ChamQ™ SYBR® color qPCR Master Mix (Vazyme, Nanjing, China) on a CFX Connect™ quantitative fluorescence PCR detection system (Bio-RAD, USA). Rat GAPDH was used for amplification as an internal control, and the relative gene expression was calculated *via* Equation $2^{-\Delta\Delta Ct}$ the primer sequences used for RT-qPCR.

Histopathologic analysis:

For histopathological analysis of bladder tissues, rats were anesthetized by administering 2 % pentobarbital sodium and then fixed on the operating table. The bladder tissues were soaked in 4 % paraformaldehyde for preservation. Routine paraffin embedding, serial sectioning and sectioning thickness of 5 μ m were performed. Hematoxylin-Eosin (HE) staining kits were obtained from Solaibao Biotechnology Co., Ltd., (Beijing, China). HE staining was observed under a 400X light microscope.

Statistical analysis:

Statistical analysis was performed using Statistical Package for the Social Sciences (SPSS) 19.0 software, and data were expressed as Means \pm Standard Error

of the Mean (SEM). One-way analysis of variance was used. $p < 0.05$ was considered as statistically significant.

RESULTS AND DISCUSSION

The effect of EA on BBB limb motor function score in SCI model rats is shown in fig. 1. Compared to the sham operation and healthy control group, the BBB limb motor function scores of the EA group and the model group were significantly lower at all evaluation time points (both $p < 0.01$); however, within 2 d after surgery, there was also no significant difference in the BBB motor function scores between the EA group and the model group; with the extension of treatment time, the BBB limb motor function score of the EA group gradually increased, and their BBB limb motor function scores were significantly better than those of the model control group from the 3rd d after treatment ($p < 0.05$), and became closer to the sham operation and healthy control group from the trend.

The results of the bladder maximum capacity test in SCI model rats are shown in Table 1. Before treatment, no significant difference in bladder maximum capacity between the model group and the EA group was observed ($p > 0.05$). Both were significantly higher than those in the sham and healthy control group on D7 after treatment. However, the EA group was still substantially higher than the sham group; it had shown a significant decrease trend compared with the sham group, and there was a statistically significant difference ($p < 0.001$). The results of filling intravesical pressure and bladder compliance tests in SCI model rats by EA are shown in Table 2. On D7 after treatment, compared with the sham group, the filling intravesical pressure in the model control and EA groups showed a statistically significant decrease. Moreover, although the filling intravesical pressure in rats after EA treatment was still lower than that in the sham group, it was significantly better than that in the model control group ($p < 0.05$). Similar improvement trends were also observed in bladder compliance, and EA treatment significantly reversed bladder compliance results in SCI model rats and was substantially different from model controls ($p < 0.05$, Table 2). The above results suggested that EA treatment can significantly improve rat's urinary and fecal disorders induced by SCI.

The results of histopathological character determination of bladder tissue in SCI model rats

are shown in fig. 2. Histopathological examination showed that the tissue structure of the healthy control group was slightly abnormal, and a minimal amount of inflammatory cell infiltration was observed in the tissue. In the sham operation group, the tissue structure was mildly abnormal, mainly as some transitional epithelial cells were vacuolated, the lamina propria was mildly thinned, and slightly increased micro vessels and inflammatory cell infiltration were observed in the tissue. In the SCI model group, the tissue structure was severely abnormal and mainly showed transitional epithelial degeneration, epithelial cell detachment, partial transitional epithelial cell

vacuolation, partial regional necrosis in the tissue, a significantly increased number of fibroblasts in the lamina propria, and inflammatory cell infiltration was observed in the tissue. While in the EA group, the tissue structure was moderately abnormal, partial transitional epithelial cell vacuolation, moderate hemorrhage in the lamina propria, lamina propria disorganization, individual regional necrosis, accompanied by fibrosis, and some inflammatory cell infiltration was observed in the tissue. Current HE staining analysis demonstrated that the EA treatment could effectively improve the histopathological characteristics of bladder tissue in the SCI mode.

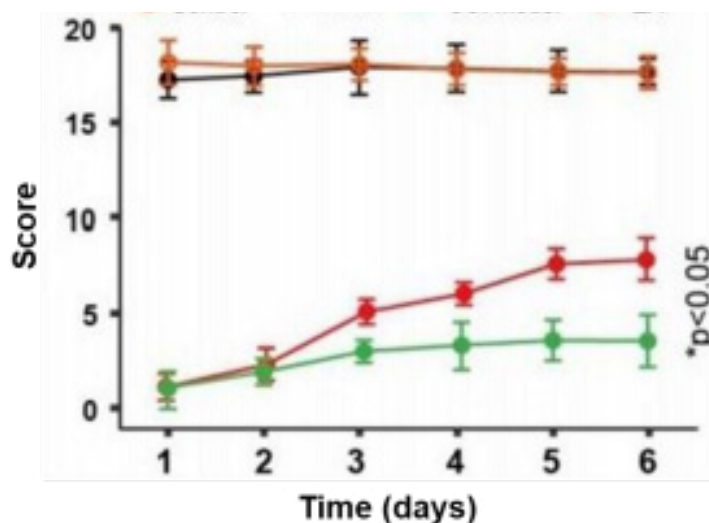


Fig. 1: BBB limb motor function score over time after SCI

Note: $p < 0.05$, compared with the SCI control group at the same period. (●): Control; (◆): Sham; (■): SCI model and (▲): EA

TABLE 1: COMPARISON OF MAXIMUM BLADDER VOLUME IN EACH GROUP AFTER TREATMENT

Group	n	Before treatment (ml)	After treatment (ml)	Difference value (ml)
Healthy	10	0.981±0.025	0.952±0.029	0.029
Sham control	10	0.901±0.011	0.911±0.015	0.01
SCI control	10	4.243±0.315	4.414±0.428	0.171
SCI+EA	10	4.182±0.297	2.922±0.512***	-1.26
F		643.238	165.873	69.453
p		0.00	0.00	0.00

Note: Data was shown as mean±SD, *** $p < 0.001$ vs. SCI control group

TABLE 2: COMPARISON OF FILLING INTERNAL BLADDER PRESSURE AND COMPLIANCE IN EACH GROUP AFTER TREATMENT

Group	n	Full bladder pressure (ml/cm H ₂ O)	Bladder compliance (ml/cm H ₂ O)
Healthy control	10	21.181±0.922	0.052±0.009
Sham	10	20.171±1.553	0.049±0.007
SCI Control	10	17.211±1.218	0.274±0.012
SCI+EA	10	19.192±1.122*	0.142±0.025**
F		7.921	218.112
p		0.00	0.00

Note: Data was shown as mean±SD, * $p < 0.05$ and ** $p < 0.01$ vs. SCI control group

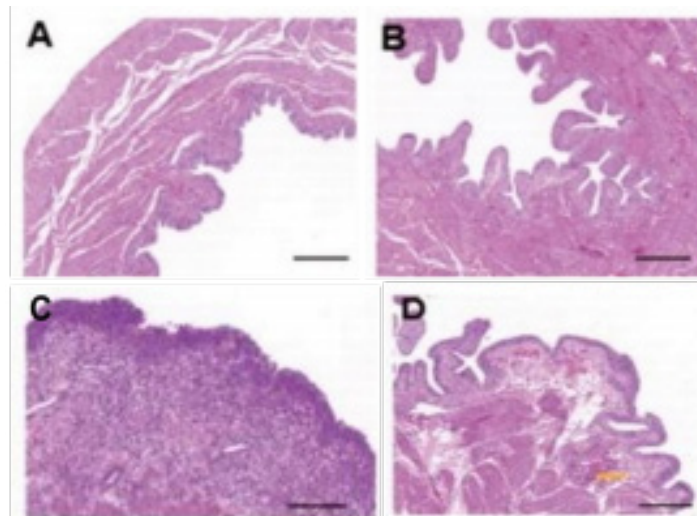


Fig. 2: HE staining bladder tissue after bladder injury in rats (400X, bar=200 μ m). (A): Healthy control; (B): Sham; (C): SCI control and (D): EA groups respectively

We measured the messenger RNA (mRNA) and protein expression of IL-1 β , IL-6, and TNF- α in the bladder tissue of rats 24 h and 7 d after SCI modeling by RT-qPCR and ELISA, respectively, and the results are shown in fig. 3 and fig. 4 accordingly. 24 h after SCI modeling, the mRNA and protein expressions of IL-1 β , IL-6, and TNF- α inflammatory factors in the bladder of rats in the model control and EA groups were significantly higher than those in the sham operation or healthy control group (all $p < 0.05$). At the same time, there was no significant difference between the two model groups. After 7 d of treatment, the expression of inflammatory factors such as IL-1 β , I-6, and TNF- α in the bladder of rats treated with EA was significantly lower than that in the SCI model group (all $p < 0.05$) but still higher than that in sham operation or healthy control group, suggesting that EA improves inflammation in the bladder of SCI model rats.

We further evaluated the effects of EA therapy on the expression of factors related to BDNF-Trk and MAPK signaling pathways, with the detection results of protein expression levels shown in fig. 5. At 7 d after the operation, the expression of BDNF protein in the sham operation and healthy control group were both significantly lower than that in the SCI model control group and EA group (both at $p < 0.01$). Moreover, the BDNF protein level in the bladder of rats treated with EA was up-regulated compared to that in the SCI control group ($p < 0.01$). Similar regulatory trends were also observed in TrkB and Protein Kinase B (AKT) changes. Compared with SC model rats, EA treatment could significantly inhibit the up-regulation of p38 MAPK protein ($p < 0.05$)

and then inhibit the activation of the inflammatory factor signaling pathway. Trends in mRNA and protein levels remained consistent (fig. 6). The above results collectively suggest that the BDNF-TrkB pathway in bladder tissues of SCI model rats treated with EA is significantly activated and up-regulated, accompanied by the inhibition of the MAPK signaling pathway, and then achieves potentially synergistic improvement of neurogenic bladder dysfunction in SCI rats.

The secondary pathological changes in the spinal cord after primary SCI will cause residual nerve cells to continue to be damaged, which is a critical reason for the difficulty in recovering limb functions after SCI^[25,26]. Reducing/inhibiting secondary SCI and protecting residual nerve cells after primary injury is essential for limb function recovery^[27,28]. Studies have confirmed that anti-edema and anti-inflammatory therapies can protect the residual nerve cells after primary injury and facilitate recovery of limb functions after SCI^[28].

Studies have demonstrated that acupuncture could reduce maximum bladder capacity by increasing detrusor contractility, relaxing the external urethral sphincter, and enhancing bladder compliance^[29]. Some researchers have found that acupuncture could improve microcirculation of injured sites in patients with SCI, enhance bladder movement and urethral sphincter relaxation and contraction function, and effectively reduce the bladder's maximum capacity^[30,31]. The mechanism of EA in the treatment of urinary retention after SCI may be related to the increase of detrusor excitability, the rise of detrusor

contraction frequency, the enhancement of bladder contraction ability, and the decrease of maximum bladder capacity, thereby reconstructing bladder function^[31]. The effect of EA on the neurogenic bladder after spinal cord injury has been confirmed clinically and experimentally^[32,33]. In this experiment, the possible protective mechanism of EA on SCI in rats can be described from the changes in the expression of inflammatory factors and related signaling pathways. The current study selected Allen's method to make the SCI model. BBB score is a commonly used neurological assessment method at present. BBB score, which includes almost all behavioral changes during the recovery of hindlimb function, is applied to assess the degree of SCI in rats and the recovery of hindlimb motor function after acupuncture treatment. The evaluation results of the BBB score showed that acupuncture therapy had a promising improvement

effect. HE analysis showed that after SCI, nerve cells were swollen and destroyed, severe infiltration of inflammatory cells was observed, the interstitial space was widened, and edema was severe. After acupuncture treatment, the above pathological changes were significantly alleviated, consistent with the BBB score. This experiment also observed that the maximum bladder capacity of each model rat was increased considerably before treatment. After treatment, the maximum bladder capacity of rats in the acupuncture group was significantly reduced, filling intravesical pressure was increased considerably, bladder compliance was significantly reduced, and the efficacy was substantially better than that of the control point group, suggesting that acupuncture can improve the bladder voiding function of detrusor areflexive rats.

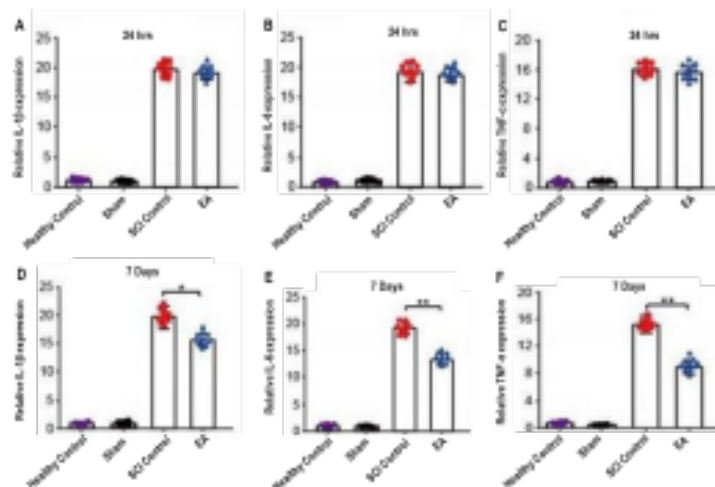


Fig. 3: EA treatment significantly decreased the expression of inflammatory factors in the bladder tissue of SCI model rats. At 24 h and 7 d, respectively, (A and D): IL-1 β ; (B and E): IL-6 and (C and F): TNF- α mRNA levels
Note: * $p < 0.05$, and ** $p < 0.01$ vs. the control group

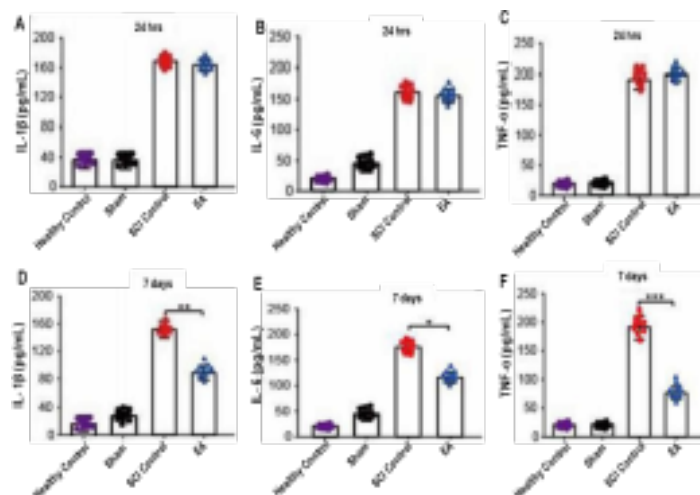


Fig. 4: EA treatment significantly decreased the expression of inflammatory proteins in the bladder tissue of SCI model rats. At 24 h and 7 d, respectively, (A and D): IL-1 β ; (B and E): IL-6 and (C and F): TNF- α protein levels
Note: * $p < 0.05$, ** $p < 0.01$ and *** $p < 0.001$ vs. the control group

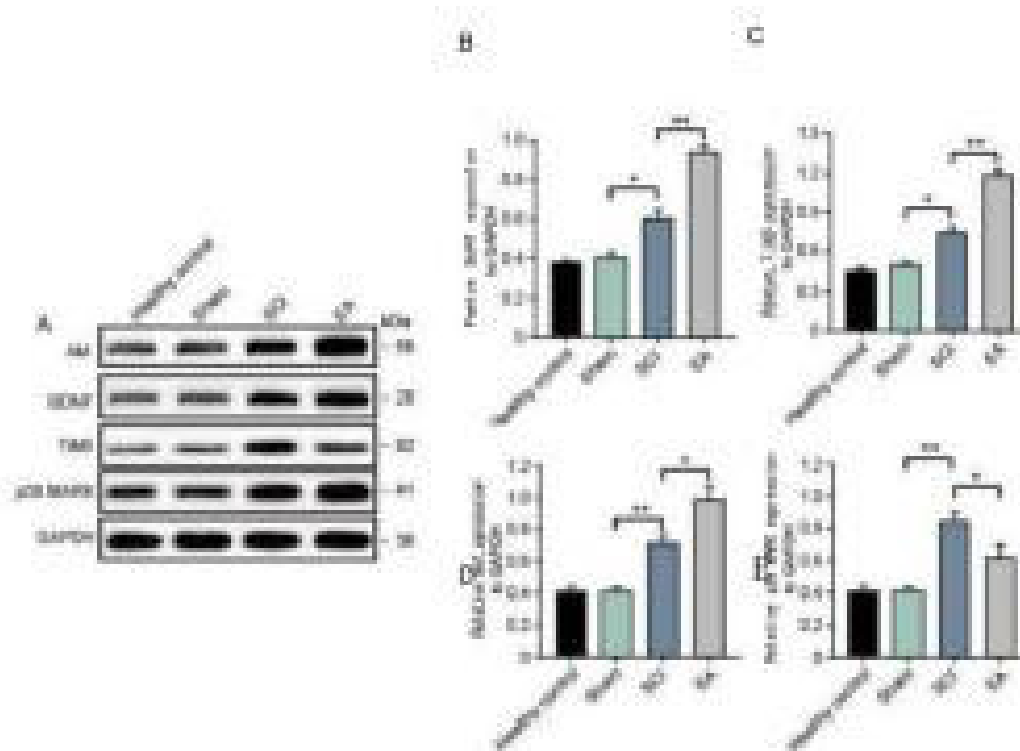


Fig. 5: EA regulates BDNF-TrkB and MAPK signaling pathways to improve SCI in model rats, (A): WB gel image and relative expression ratio; (B): BDNF; (C): TrkB; (D): Akt and (E): p38 MAPK
Note: * $p < 0.05$ and ** $p < 0.001$ vs. control group

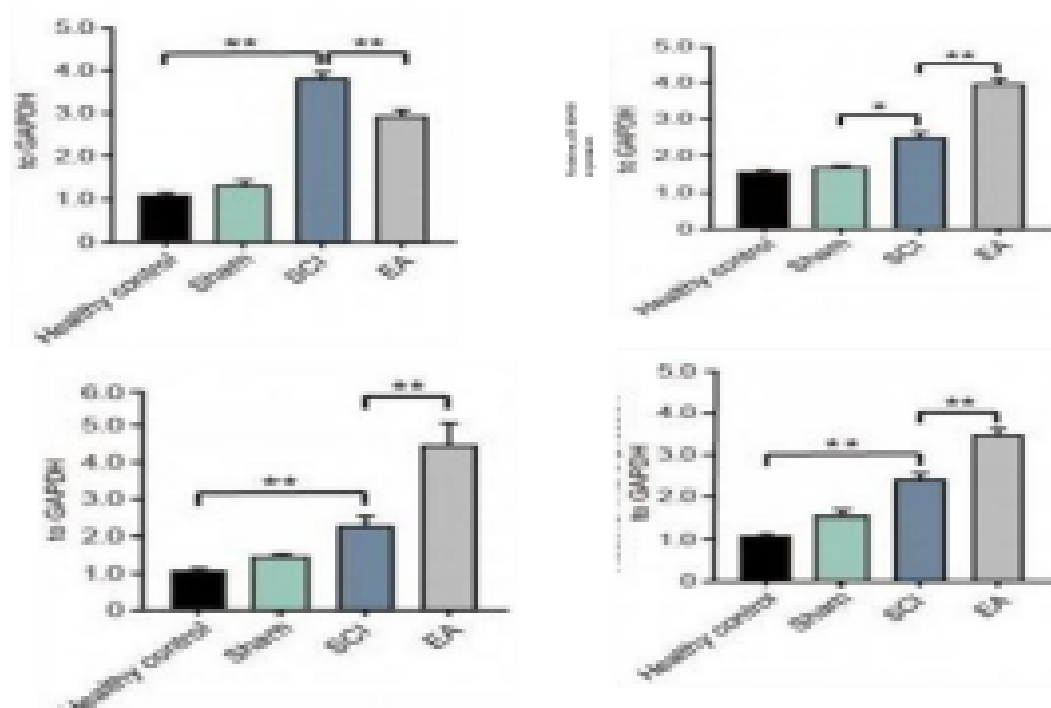


Fig. 6: EA regulates BDNF-TrkB and MAPK signaling pathways to improve SCI in model rats. Relative mRNA expression ratio, (A): BDNF; (B): TrkB; (C): Akt and (D): p38 MAPK
Note: * $p < 0.05$ and ** $p < 0.001$ vs. control group

It has been reported that after SCI, many proinflammatory factors such as IL-1, IL-6, and TNF- α are produced locally in the body of injury, which has also been confirmed in this study^[34]. These produced

inflammatory factors will recruit inflammatory cells such as neutrophils, macrophages, monocytes, and T lymphocytes to adhere and metastasize to the injury site and activate, and excessively accumulated

inflammatory cells can produce a severe secondary inflammatory cascade by secreting larger amounts of pro-inflammatory factors, which can activate neutrophils and lymphocytes, increase vascular endothelial cell permeability, damage residual neurons and destroy axonal myelin sheaths, axons and gradually degrade and necrosis^[35]. In this study, we found that after SCI modeling was completed, a lot of inflammatory factors were released locally in the bladder of model rats, and the results of RT-qPCR and ELISA detection revealed that IL-1 β , IL-6 and TNF- α were increased; after acupuncture treatment, IL-1 β , IL-6 and TNF- α in the bladder were all obviously decreased, showing a better trend of improvement, suggesting that acupuncture therapy can inhibit many pro-inflammatory factors released locally in the bladder of SCI model and has an anti-inflammatory effect, which has potential value for the treatment of SCI, but it still necessary to further verify the efficacy differences and cure of SCI models under different conditions.

BDNF binds to TrkB transmembrane receptors and forms a dimeric complex structure that promotes tyrosine receptor residues in the intracellular region of the target cell to undergo or accelerate autophosphorylation, thereby activating downstream related signaling pathways, including Phosphatidylinositol 3-Kinase(PI3K)/AKT, MAPK signaling pathways, promoting the transcription of the transcription factor, CREB, regulating neural cell survival, proliferation, and synaptic remodeling, and promoting neuronal cell growth after SCI, thereby improving neuronal cell function, promoting nervous system repair, and improving limb motor function^[36,37]. In this study, 7 d after surgery, compared to the model group, expression of TrkB and the BDNF in bladder tissues of rats in the EA group were up-regulated relative to the control group ($p < 0.01$).

MAPK signaling pathway plays an essential role in cell differentiation and proliferation in the CNS and the pathophysiology of SCI^[38]. The MAPK pathway is often detected by the indicator of p38 MAPK^[39-41]. p38 and JNK MAPK signaling pathways are associated with inflammation and stress responses; specifically, p38 MAPK is activated after cell injury stress and activates a series of signaling pathways and proteins downstream of inflammation-related, injured spinal cord neurons, astrocytes and macrophages to increase the expression of p38 MAPK, and down-

regulation of p38 MAPK expression after SCI can promote SCI functional recovery^[42-46]. In this study, at 7 d after surgery, the expression of p38 MAPK protein in the bladder of rats in the EA group was down-regulated compared to the SCI control group ($p < 0.01$).

In summary, acupuncture therapy may be associated with BDNF/TrkB and MAPK pathways in ameliorating urinary and fecal disorders in rats with neurogenic bladder after SCI. The significant up-regulation of BDNF/TrkB and inhibition of MAPK inflammation-related signaling pathways can improve the therapeutic efficacy of SCI accompanied by neurogenic disorders of the bladder.

Funding:

This work was sponsored in part by The National Science Foundation of China (No: 82174480).

Conflict of interests:

The authors declared no conflict of interests.

RREFERENCES

1. Mugge L, Dang DD, Dang J, Leiphart J. Acute spinal cord injury due to epidural lipomatosis without osseous injury. *Cureus* 2022;14(5).
2. Hamid R, Averbeck MA, Chiang H, Garcia A, Al Mousa RT, Oh SJ, *et al.* Epidemiology and pathophysiology of neurogenic bladder after spinal cord injury. *World J Urol* 2018;36:1517-27.
3. Jeong HJ, Yun Y, Lee SJ, Ha Y, Gwak SJ. Biomaterials and strategies for repairing spinal cord lesions. *Neurochem Int* 2021;144:104973.
4. Tran AP, Warren PM, Silver J. The biology of regeneration failure and success after spinal cord injury. *Physiol Rev* 2018;98(2):881-917.
5. Havelikova K, Smejkalova B, Jendelova P. Neurogenesis as a tool for spinal cord injury. *Int J Mol Sci* 2022;23(7):3728.
6. Freyermuth-Trujillo X, Segura-Urbe JJ, Salgado-Ceballos H, Orozco-Barrios CE, Coyoy-Salgado A. Inflammation: A target for treatment in spinal cord injury. *Cells* 2022;11(17):2692.
7. Chen SF, Lee YK, Kuo HC. Satisfaction with urinary incontinence treatments in patients with chronic spinal cord injury. *J Clin Med* 2022;11(19):5864.
8. Tremont JN, Cook N, Murray LH, Udekwu PO, Motameni AT. Acute traumatic spinal cord injury: Implementation of a multidisciplinary care pathway. *J Trauma Nurs* 2022;29(4):218-24.
9. Zipser CM, Cragg JJ, Guest JD, Fehlings MG, Jutzeler CR, Anderson AJ, *et al.* Cell-based and stem-cell based treatments for spinal cord injury: Evidence from clinical trials. *Lancet Neurol* 2022;21(7):659-70.
10. Lavrov I, Islamov R. Implementing Principles of neuroontogenesis and neuroplasticity for spinal cord injury therapy. *Front Biosci (Landmark Ed)* 2022;27(5):163.

11. Behl T, Kotwani A. Downregulated brain-derived neurotrophic factor-induced oxidative stress in the pathophysiology of diabetic retinopathy. *Can J Diabetes* 2017;41(2):241-6.
12. G eral C, Angelova A, Lesieur S. From molecular to nanotechnology strategies for delivery of neurotrophins: Emphasis on Brain-Derived Neurotrophic Factor (BDNF). *Pharmaceutics* 2013;5(1):127-67.
13. Liang J, Deng G, Huang H. The activation of BDNF reduced inflammation in a spinal cord injury model by TrkB/p38 MAPK signaling. *Exp Ther Med* 2019;17(3):1688-96.
14. Mantilla CB, Gransee HM, Zhan WZ, Sieck GC. Motoneuron BDNF/TrkB signaling enhances functional recovery after cervical spinal cord injury. *Exp Neurol* 2013;247:101-9.
15. Liang W, Han B, Hai Y, Liu Y, Liu X, Yang J, *et al.* The role of microglia/macrophages activation and TLR4/NF- B/MAPK pathway in distraction spinal cord injury-induced inflammation. *Front Cell Neurosci* 2022;16:926453.
16. Xia M, Zhang Y, Wu H, Zhang Q, Liu Q, Li G, *et al.* Forsythoside B attenuates neuro-inflammation and neuronal apoptosis by inhibition of NF- B and p38-MAPK signaling pathways through activating Nrf2 post spinal cord injury. *Int Immunopharmacol* 2022;111:109120.
17. Kim EK, Choi EJ. Compromised MAPK signaling in human diseases: An update. *Arch Toxicol* 2015;89:867-82.
18. Knebel B, Lehr S, Hartwig S, Haas J, Kaber G, Dicken HD, *et al.* Phosphorylation of Sterol Regulatory Element-Binding Protein (SREBP)-1c by p38 kinases, ERK and JNK influences lipid metabolism and the secretome of human liver cell line HepG2. *Arch Physiol Biochem* 2014;120(5):216-27.
19. Kasuya Y, Umezawa H, Hatano M. Stress-activated protein kinases in spinal cord injury: Focus on roles of p38. *Int J Mol Sci* 2018;19(3):867.
20. Yue J, L pez JM. JNK does not regulate meiotic progression in *Xenopus* oocytes: The strange case of pJNK and pERK. *Dev Biol* 2016;416(1):42-51.
21. Li S, Zhou J, Zhang J, Wang D, Ma J. Construction of rat spinal cord injury model based on Allen's animal model. *Saudi J Biol Sci* 2019;26(8):2122-6.
22. Basso DM, Beattie MS, Bresnahan JC. A sensitive and reliable locomotor rating scale for open field testing in rats. *J Neurotrauma* 1995;12(1):1-21.
23. Zhang Y, Zhang Z, Ai K, Bao Q, Li J, Kuang J. Neurogenic bladder following spinal cord injury: A rat model. *Chin J Rehab Med* 2014;6:542-6.
24. Liu XM, Ming XU, Zhang H, Kun AI, Deng SF, Yu YH. Effects of electroacupuncture on urodynamics, intramedullary apoptosis and bidirectional regulation of neurotrophic factors in neurogenic bladder rats after supersacral spinal cord injury. *World J Acupunct Moxib* 2021;31(2):121-8.
25. Gu G, Ren J, Zhu B, Shi Z, Feng S, Wei Z. Multiple mechanisms of curcumin targeting spinal cord injury. *Biomed Pharmacother* 2023;159:114224.
26. Chu XL, Song XZ, Li Q, Li YR, He F, Gu XS, *et al.* Basic mechanisms of peripheral nerve injury and treatment *via* electrical stimulation. *Neural Regen Res* 2022;17(10):2185-93.
27. Gao R, Li X, Xi S, Wang H, Zhang H, Zhu J, *et al.* Exogenous neuritin promotes nerve regeneration after acute spinal cord injury in rats. *Hum Gene Ther* 2016;27(7):544-54.
28. Liu G, Zhao Z, Wang H, Hao C, Wang W, Zhang C, *et al.* Therapeutic efficacy of human mesenchymal stem cells with different delivery route and dosages in rat models of spinal cord injury. *Cell Transplant* 2022;31:09636897221139734.
29. Fujishiro T, Takahashi S, Enomoto H, Ugawa Y, Ueno S, Kitamura T. Magnetic stimulation of the sacral roots for the treatment of urinary frequency and urge incontinence: An investigational study and placebo controlled trial. *J Urol* 2002;168(3):1036-9.
30. Yang YJ, Kim YS, Shin MS, Chang HK, Lee TH, Sim YJ, *et al.* Effects of acupuncture on the intrastriatal hemorrhage-induced caspase-3 expression and newly cell birth in rats. *Neurol Res* 2007;29:65-71.
31. Kjell J, Olson L. Rat models of spinal cord injury: From pathology to potential therapies. *Dis Model Mech* 2016;9(10):1125-37.
32. Zhengfei L, Zhang R, Guorui Z, Kuang Y. Electroacupuncture in the treatment of neurogenic urine retention through autophagy mediated by AMPK/mTOR pathway. *J Central South Univ Med Sci* 2022:488-96.
33. Mazensky D, Flesarova S, Sulla I. Arterial blood supply to the spinal cord in animal models of spinal cord injury. A review. *Anat Rec* 2017;300(12):2091-106.
34. Garcia E, Aguilar-Cevallos J, Silva-Garcia R, Ibarra A. Cytokine and growth factor activation *in vivo* and *in vitro* after spinal cord injury. *Mediators Inflamm* 2016;2016(1):9476020.
35. Ak H, G l sen  , Karaaslan T, Alaca  , Candan A, Ko ak H, *et al.* The effects of caffeic acid phenethyl ester on inflammatory cytokines after acute spinal cord injury. *Ulus Travma Acil Cerrahi Derg* 2015;21(2):96-101.
36. Sanchez-Huertas C, Rico B. CREB-dependent regulation of GAD65 transcription by BDNF/TrkB in cortical interneurons. *Cereb Cortex* 2011;21(4):777-88.
37. Zhou X, Xiao H, Wang H. Developmental changes of TrkB signaling in response to exogenous brain-derived neurotrophic factor in primary cortical neurons. *J Neurochem* 2011;119(6):1205-16.
38. Zhang H, Wang Y. Identification of molecular pathway changes after spinal cord injury by microarray analysis. *J Orthop Surg Res* 2016;11(1):101.
39. Rubinfeld H, Seger R. The ERK cascade: A prototype of MAPK signaling. *Mol Biotechnol* 2005;31:151-74.
40. Lee JY, Chung H, Yoo YS, Oh YJ, Oh TH, Park S, *et al.* Inhibition of apoptotic cell death by ghrelin improves functional recovery after spinal cord injury. *Endocrinol* 2010;151(8):3815-26.
41. Zhang S, Xia YY, Lim HC, Tang FR, Feng ZW. NCAM-mediated locomotor recovery from spinal cord contusion injury involves neuroprotection, axon regeneration, and synaptogenesis. *Neurochem Int* 2010;56(8):919-29.
42. Saklatvala J. The p38 MAP kinase pathway as a therapeutic target in inflammatory disease. *Curr Opin Pharmacol* 2004;4(4):372-7.
43. Ghasemlou N, Lopez-Vales R, Lachance C, Thuraisingam T, Gaestel M, Radzioch D, *et al.* Mitogen-activated protein kinase-activated protein Kinase 2 (MK2) contributes to secondary damage after spinal cord injury. *J Neurosci* 2010;30(41):13750-9.
44. Wang J, Su B, Zhu H, Chen C, Zhao G. Protective effect of geraniol inhibits inflammatory response, oxidative stress and apoptosis in traumatic injury of the spinal cord through

modulation of NF- κ B and p38 MAPK. *Exp Ther Med* 2016;12(6):3607-13.

45. Tran HT, Sanchez L, Brody DL. Inhibition of JNK by a peptide inhibitor reduces traumatic brain injury-induced tauopathy in transgenic mice. *J Neuropathol Exp Neurol* 2012;71(2):116-29.
46. Martini AC, Forner S, Koepp J, Rae GA. Inhibition of spinal c-Jun-NH₂-Terminal Kinase (JNK) improves locomotor activity of spinal cord injured rats. *Neurosci Lett* 2016;621:54-61.

This is an open access article distributed under the terms of the Creative Commons Attribution-NonCommercial-ShareAlike 3.0 License, which allows others to remix, tweak, and build upon the work non-commercially, as long as the author is credited and the new creations are licensed under the identical terms

This article was originally published in a special issue, "Drug Discovery and Repositioning Studies in Biopharmaceutical Sciences" Indian J Pharm Sci 2024;86(4) Spl Issue "206-216"